Journal of the European Ceramic Society **8** (1991) 233–241

Proposal of a Composition Model for Commercial AlN Powders

E. Ponthieu,‡ P. Grange, B. Delmon

Université Catholique de Louvain, Unité de Catalyse et de Chimie des Matériaux Divisés, 2, Place Croix du Sud, 1348 Louvain-la-Neuve, Belgium

&

L. Lonnoy, L. Leclercq, R. Bechara, J. Grimblot

Université des Sciences et des Techniques de Lille Flandre-Artois, Laboratoire de Catalyse hétérogène et homogène, Bât. C3, 59655 Villeneuve d'Ascq Cédex, France

(Received 27 December 1990; accepted 20 June 1991)

Abstract

Commercially available AlN powders were submitted to bulk and superficial characterisations. XPS analysis of as-received samples shows the presence of an important quantity of superficial oxygen. The detected nitrogen whose N_{1s} binding energy is 396·9 eV (±0·3 eV) can be identified as a nitride species. After a rare gas bombardment devoted to the progressive removal of the uppermost layers, the initial compounds AlO_xN_y (with $1{\cdot}3 \geq x \geq 0{\cdot}7$ and $0{\cdot}6 \geq y \geq 0{\cdot}4$, depending on the origin of the samples) exhibited an average formula $AlO_{0{\cdot}5}N_{0{\cdot}5}$. IR spectroscopy, coupled with a mixed vacuum-heating system, and the thermogravimetric analysis emphasise the existence of superficial OH species. In contrast, the crystallographic analysis displays solely an AlN hexagonal structure for all the samples. On the basis of these results, a model based on a composition gradient from the inner core to the superficial layers is proposed. It is assumed that an AlN core is surrounded by an oxynitride phase ($Al_{0{\cdot}05}N_{0{\cdot}6}$) which is recovered by hydroxylated species in a phase close to $Al(OH)_3$ and/or AlOOH.

Diverse kommerziell erhältliche AlN-Pulver wurden auf ihre Volumen- und Oberflächeneigenschaften hin untersucht. XPS Analysen der erhaltenen Pulver konnten signifikante Mengen an oberflächlich gebundenem Sauerstoff nachweisen. Stickstoff, dessen N_{1s}-Bindungsenergie bei 396·9 eV (±0·3 eV) liegt, konnte als Nitrid nachgewiesen werden. Nach einem Edelgassputterprozeß, der die oberflächliche Schicht entfernte, veränderte sich die ursprüngliche Zusammensetzung des AlO_xN_y (mit $1{\cdot}3 \geq x \geq 0{\cdot}7$ und $0{\cdot}6 \geq y \geq 0{\cdot}4$, je nach Ausgangsmaterial) und es ergab sich für die Zusammensetzung ein mittlerer Wert von $AlO_{0{\cdot}5}N_{0{\cdot}6}$. IR-Spektroskopie in Verbindung mit einer Vakuumapparatur mit Ausheizmöglichkeit und thermogravimetrischer Analyse konnte die Anwesenheit oberflächlicher OH-Gruppen nachweisen. Im Gegensatz dazu ergab die kristallographische Untersuchung an allen Proben nur die hexagonale AlN–Struktur. Aufgrund dieser Ergebnisse wird eine modellhafte Betrachtung vorgeschlagen, die von einem Gradienten bzgl. der Zusammensetzung vom Zentrum des Korns zur äußeren Randschicht ausgeht. Dabei wird angenommen, daß ein Kern von AlN von einer Schale oxinitridischer Zusammensetzung ($AlO_{0{\cdot}5}N_{0{\cdot}6}$) umgeben ist, die an der Oberfläche durch Hydroxylgruppen abgesättigt wird und seitens der Zusammensetzung nahe an $Al(OH)_3$ und/oder AlOOH liegt.

Des poudres commerciales d'AlN furent caractérisées en surface et dans la masse. L'analyse XPS des échantillons tels quels montre la présence d'une importante quantité d'oxygène en surface. L'énergie de liaison du pic N_{1s} (396·9 eV ± 0·3 eV) est typique d'espèces de type nitrure. Un bombardement sous

‡On leave at the Université des Sciences et des Techniques de Lille Flandre-Artois, Laboratoire de Catalyse hétérogène et homogène, bât. C3, 59655 Villeneuve d'Ascq Cédex, France.

Journal of the European Ceramic Society 0955-2219/91/$3.50

particules de gaz rare, destiné à décaper progressivement les couches les plus externes, provoque une homogénéisation de la composition superficielle des grains (avant décapage: AlO_xN_y, avec $1{\cdot}3 \geq x \geq 0{\cdot}7$ et $0{\cdot}6 \geq y \geq 0{\cdot}4$; après décapage: $AlO_{0{\cdot}5}N_{0{\cdot}6}$). La spectroscopie infrarouge, couplée avec un système de chauffage sous vide, et la thermogravimétrie ont permis de montrer l'existence d'espèces hydroxylées en surface. Par contre, pour la diffraction des rayons X, seule une structure AlN hexagonale apparaît pour tous les solides. En conséquence, un modèle basé sur un gradient de composition entre le centre et les couches superficielles est proposé. On suppose qu'un noyau d'AlN est entouré par une phase oxynitrure ($AlO_{0{\cdot}5}N_{0{\cdot}6}$), laquelle est recouverte par des espèces hydroxylées du type $Al(OH)_3$ et/ou AlOOH.

1 Introduction

Aluminium nitride (AlN) ceramic is an attractive substrate for applications in today's electronic packaging, due to its unique physical properties, i.e. a high thermal conductivity (91–190 W/m K) close to metals,[1,2] a high electrical resistivity (10^{11}–$10^{14}\,\Omega$cm), and a thermal expansion coefficient ($4{\cdot}3$–$4{\cdot}5 \times 10^{-6}$°C) matched to the semiconductor silicon. These physical properties are superior to those of alumina ceramics and more or less equivalent to those of beryllia ceramics. However, BeO is generally considered to be highly toxic and its use should be limited.

The physical properites of AlN are significantly influenced by its chemical purity and density. For example, the AlN thermal conductivity is strongly affected when oxygen is incorporated within the structure, so that the theoretical value (320 W/m K) is never attained.[3] It was established that the thermal conductivity of AlN decreases as the oxygen content increases.[4] The presence of oxygen generates other interesting features, such as an acceleration of the densification of hot-pressed AlN substrates, and the improvement of the mechanical strength of sintered AlN.[5] The situation is more different still when oxygen-containing additives are mixed with AlN.[6,7]

The adhesion properties of AlN, which are very important for the potential uses of AlN substrates, are also largely dependent on the chemical nature of the superficial species present on the powder grains. Whereas aluminium hydroxide has deleterious effects on the metal adhesion to ceramics,[2] Al_2O_3 layers can improve the adhesion strength of thin copper films on AlN ceramic substrates.[2,8]

The reactivity of AlN towards any oxygen-containing environments, such as moist air,[9–12] H_2O,[10,13–15] O_2,[5,16–20] SiO,[21] etc., has been widely reported in the literature.

The behaviour of AlN ceramics under wet air or oxygen showed that the AlN surfaces are significantly altered by these treatments.[9] The formation of superficial AlOOH and $Al(OH)_3$ was emphasised.[9,11] The growth kinetics of these layers is influenced by the pressure and the temperature of the treating atmosphere.[9] The surface morphology was also found to change and the insulation characteristics were degraded.[10] The kinetics of oxidation by air was shown to be promoted by water vapour.[12]

The degradation in aqueous environments at room temperature was shown to consume 80% of the AlN in 24 h.[13] An amorphous oxyhydroxide shell, of probable formula AlOOH, initially appears, whereas after 16 h a crystalline phase, bayerite $Al(OH)_3$, becomes predominant.[14] The authors assumed that this process occurs in terms of a shrinking-core model.[14] In addition, elevated pH levels generate a more severe moisture attack on AlN.[15] These studies, which are motivated by the possible use of AlN in aqueous suspensions for both economic reasons and control of colloidal processing, demonstrate that the use of H_2O in the colloidal ceramic processing is not viable, especially if contact times are of the order of hours.

In contrast, Al_2O_3 is mostly found to be the end product of a thermal oxidation treatment in dry air.[16,20] The oxidation, which is initiated at 700°C, leads first to the formation of an intermediate state, represented by AlON. The oxynitride, which appears before the formation of Al_2O_3 at 900°C, persists at higher temperatures, forming an interfacial layer between oxide and nitride. The oxide layer, which is relatively thin (1–2 μm thick),[18] is known to be an effective protection for AlN powders against any oxidising medium.[9,10] Even at 1450°C, oxidation is very slow, because the oxide coating forms a protective barrier. Suryanarayana[17] had also proved that the thermal oxidation kinetics of AlN is particle-size dependent. The lower the mean particle size, the faster the initial oxidation step. Identically, the sensitivity towards oxidation of a densified AlN compact is inferior to that of fine grain powders.[11] Those densified AlN-based ceramics present indeed a good oxidation resistance in air or in oxygen, up to 1100°C[22,23] or 1300°C.[19]

Although the behaviour of AlN under thermal, hydrothermal and aqueous environments has been widely studied, very few papers relate to the influence of ambient conditions during storage of

nitride powders. For comparison, an XPS (X-ray photoelectron spectroscopy) investigation[24] of as-received Si_3N_4 powders has established that in such conditions, the surface-layer composition is intermediate between silica and silicon oxynitride, demonstrating that nitride materials are thermodynamically unstable, even when exposed to ambient conditions. Similar conclusions have already been obtained[25] on protective Al_2O_3 layers on aluminium which are altered by storing oxidised aluminium films in a normal laboratory environment.

To the knowledge of the present authors, no work has tried until now to present an insight on the superficial and bulk properties of as-received AlN powders. However, the features of the starting powders are probably some of the most important parameters conditioning the final properties of a ceramic material. For this study, several characterisation techniques were used: XPS, X-ray powder diffraction (XRD), Fourier-Transform infrared spectroscopy (FTIR) and thermogravimetric analysis (TGA). The data obtained are fitted to a comparison model which describes the inhomogeneous nature of the samples, i.e. the existence of a thin outer shell of hydrolysis product surrounding an Al oxynitride-like phase, whereas the core of the materials consists of unreacted AlN.

2 Experimental Procedure

2.1 Specimens

Commercially available AlN powders from different origins were used in this study. Their characteristics (chemical analysis, mean diameter, specific area and density), which were provided by the suppliers, are detailed in Table 1. The mean diameter of the samples extends approximately from 1 to 50 μm. Their purity is generally satisfactory, the main impurity source being carbon. Three AlN powders (ART AG 35, 75, 250) contain Y_2O_3 additives, in quantities varying from 3 to 5 wt%.

2.2 XRD

The diffraction patterns were obtained with a Siemens D500 apparatus, with a copper anticathode and a secondary monochromator. Tension was adjusted at 50 kV and current at 35 mA. Samples were analysed in a powder form.

2.3 XPS

The surface analysis was conducted on a Leybold Hereaus LHS10 apparatus. Irradiation of the samples is performed under ultra-high vacuum conditions (10^{-8}–10^{-9} torr) with AlK_α X-ray source ($h\nu = 1486{\cdot}6$ eV). The source power was maintained at 299 W (23 mA, 13 kV). The kinetic energies of the emitted photoelectrons were analysed with a hemispherical detector. The spectra were taken using a differential pass energy ($\Delta E/E$) of 50 for the analyser. The Al_{2p} reference, whose binding energy (BE) was fixed at 73·8 eV,[26] has allowed the determination of the binding energies (BE) of the O_{1s}, N_{1s}, C_{1s} levels. The angle between the sample surface and the analyser is a constant (90°) for the apparatus. Solids were simply pressed on an indium plate with the help of a spatula and a grip. Samples were analysed before and after rare gas (Ar, Ne) etching in the preparation chamber. Rare gas bombardment was used for depth profiling. The discharge potential and current were fixed respectively to 3 keV and 8 mA, while the discharge tension was higher in the case of argon etching (600 V) than for neon etching (490 V). It is assumed that in these conditions about one monolayer (2 Å) is etched every 30 s from the surface. A thermal treatment of the A2B solid was also conducted in the analyser chamber up to 600°C. At this temperature, the sample was exposed to an oxygen leak (10^{-6} torr). In this case, the solid was prepared differently: a paste composed of AlN powder and ethanol was 'applied' to the surface of a stainless steel sample holder. Atomic ratios (O/Al,

Table 1. Main characteristics of the commercial AlN powders

Type	*Chemical analysis (wt%)*			$D_{50\%}$[a] (μm)	SA[b] ($m^2 g^{-1}$)
	N	*O*	*C*		
ART (USA)					
A100	33·4	1·0	0·07	2·5–4·0	2·0–5·0
A200	32·9	1·3	0·10	3·3	3·7
AG35	—	—	—	—	0·5
AG75	—	—	—	—	0·2
AG250	—	—	—	—	0·1
Atochem (France)					
A4	33·0	1·1	<0·1	2·4	2·4
A2B	32·9	1·2–1·5	<0·1	2·2	3·5
A2C	32·9	1·2–1·5	<0·1	1·4	3·5
Sumitomo (Japan)					
ANS21	33·5	1·2	0·07	1·1	3·4
ANS210	33·2	1·0	0·07	2·6	3·0
ANH20	32·9	1·2	0·07	3·0	3·2
Starck (UK)					
ST-A	31·5	1·5	0·1	2·5–4·0	1·5–3·0
ST-B	32·0	2·0	0·1	1·0–2·5	3·0–6·0
ST-C	29·5	2·5	0·1	0·8–1·3	4·0–8·0
ST-D	33·0	0·9	0·08	2·0–4·0	0·5–3·0

[a] Mean diameter.
[b] Specific area determined by BET methods.

N/Al, C/Al) were calculated from the corresponding XPS intensity ratios using the Scofield[27] cross-section values and assuming that the mean electron escape depth is proportional to $(KE)^{0.8}$, with KE referring to the kinetic energy of the corresponding photoelectrons. Chemical formula in the exposed surface layers were deduced from these atomic ratios.

2.4 FTIR

Infrared spectra were recorded at 400–4000 cm^{-1} on a Brucker IFS 88 Fourier Transform spectrophotometer. In a first step, the nitride powders were mixed with spectroscopic grade potassium bromide (99:1 by weight) and pellets were made at a pressure of 3 T/cm^2 for 30 s. The dispersion in KBr allows for a better resolution of broad peaks, which otherwise would be unusable. The second step consisted in measuring the IR absorbance directly through auto-supported AlN pellets (prepared identically as previous ones). These pellets were introduced in Pyrex cells where a heating treatment was carried out under a vacuum of 10^{-6} torr in order to clean the surface. Finally, a baseline correction treatment was applied to all IR spectra.

2.5 TGA

Thermogravimetric analysis was performed with the help of a Setaram MTB 10-8 microbalance. The system permits the recording of any weight change during the thermal treatment of a small quantity of sample. The He flow was adjusted at 40 ml/min.

3 Results

3.1 XRD

AlN powders, which do not contain Y_2O_3 additives, present XRD spectra (Fig. 1) with a unique wurtzite-type hexagonal structure. If yttria is added as sintering aid (Fig. 1), two minority crystallographic phases appear besides AlN: on the one hand, an yttria phase and on the other hand, a mixed $Y_2Al_4O_9$ phase.

3.2 XPS

Figure 2 presents the typical X-ray photoelectron spectrum of a powder (here, sample A2B from Atochem, France), before and after neon etching. After expanding the scale, it appears that the various lines are highly symmetrical and this symmetry is not perturbed during the etching procedure. The oxygen Auger transition peaks (O_{KVV}) are always present on the examined samples whereas the N_{KVV} peaks are

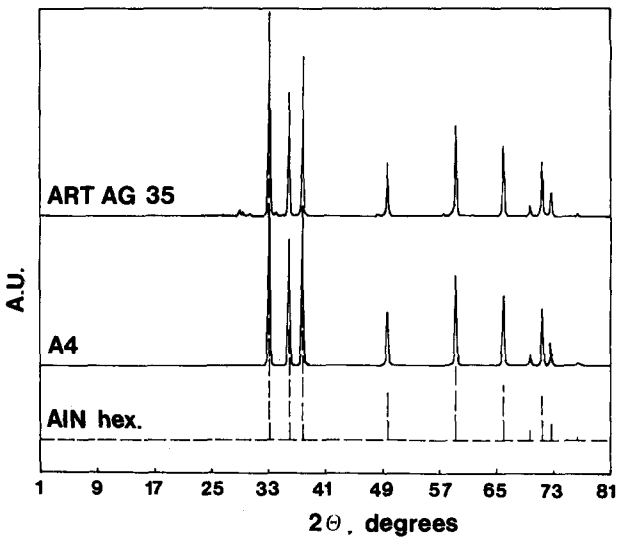

Fig. 1. XRD spectra of both yttrium-free (A4B) and yttrium-containing (ART AG35) AlN powders.

detected generally only after ion etching. In order to fully understand these results, it is important to note that Auguer electrons (with low kinetic energies) are known to come from the uppermost layers of analysed particles.

Surface stoichiometries derived from the quantitative analysis, are reported, before and after etching, in Table 2. BE values which are more or less identical for all the samples (i.e. 531·8 eV ± 0·3 eV for O_{1s} and 396·9 eV ± 0·3 eV for N_{1s}) are found to be independent from the etching procedure. Full width at half maximum (FWHM) of superficial elements vary in opposite directions as a result of the bombardment: the O_{1s} width decreases whereas the

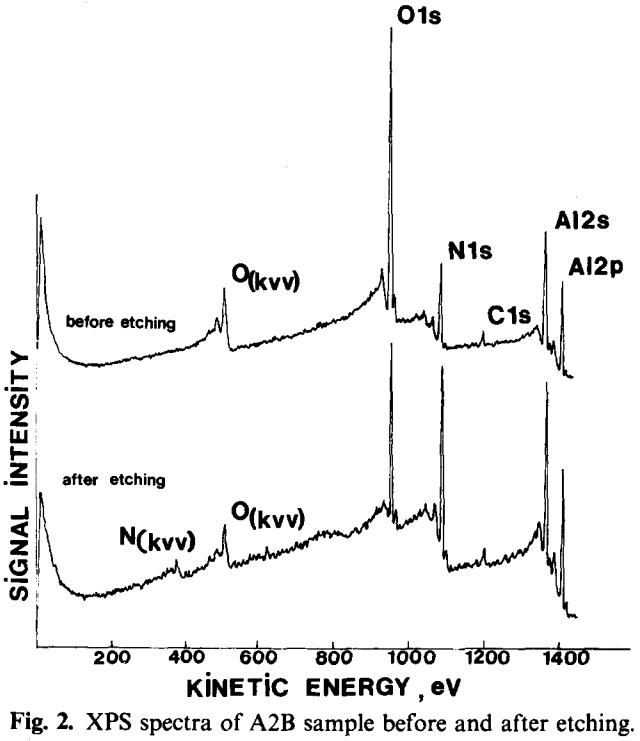

Fig. 2. XPS spectra of A2B sample before and after etching.

Table 2. XPS analysis of the commercial AlN samples

Type	*Chemical formula*	
	Before etching	*After etching*
Argon etching		
A100	$AlO_{1.29}N_{0.58}$	$AlO_{0.72}N_{0.51}$
A200	$AlO_{1.19}N_{0.51}$	$AlO_{0.76}N_{0.46}$
ANH20	$AlO_{0.81}N_{0.45}$	$AlO_{0.61}N_{0.55}$
ANS21	$AlO_{0.85}N_{0.54}$	$AOl_{0.33}N_{0.74}$
ANS210	$AlO_{0.82}N_{0.51}$	$AlO_{0.55}N_{0.64}$
Neon etching		
A2B	$AlO_{1.2}N_{0.4}$	$AlO_{0.5}N_{0.6}$
A4	$AlO_{1.3}N_{0.4}$	$AlO_{0.58}N_{0.56}$
ST-A	$AlO_{0.77}N_{0.6}$	$AlO_{0.54}N_{0.61}$
ST-B	$AlO_{0.95}N_{0.62}$	$AlO_{0.69}N_{0.6}$
ST-C	$AlO_{1.0}N_{0.62}$	$AlO_{0.71}N_{0.52}$
ST-D	$AlO_{1.19}N_{0.43}$	$AlO_{0.58}N_{0.57}$

N_{1s} and Al_{2p} ones increase. Literature data concerning the N_{1s} BE values show some variation between different sources.[9,16,28-30] Values close to those obtained in the present study are proposed by some authors.[28-30] On a quantitative point of view, oxygen levels appear to be very high. After etching, there is a better homogeneity between all the calculated chemical formula so that an average formula can be proposed for etched samples: AlO_xN_y, with $0{\cdot}7 \geq x \geq 0{\cdot}5$ and $0{\cdot}6 \geq y \geq 0{\cdot}5$. If longer etching times ($t > 20$ min) are used, there is no further significant changes in the above-mentioned formula.

Another identical study was also conducted for yttrium-containing powders (Table 3). In this case, an argon bombardment for 20 min leads to a similar

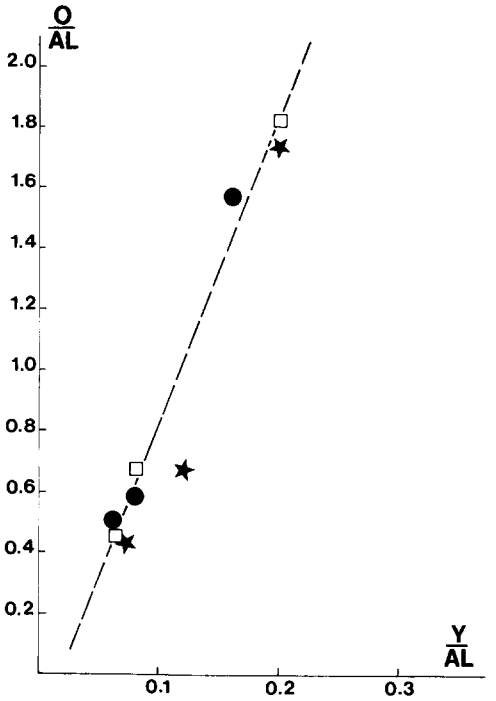

Fig. 3. Superficial yttrium content versus oxygen content. □, AG35; ●, AG75; ★, AG250.

formula to that for yttrium-free samples. Superficial Y/Al ratios are significantly larger than the bulk ones. Moreover, these ratios are well correlated to superficial O/Al molar ratios, as is clearly indicated in Fig. 3. It is estimated that a 20-min rare gas bombardment removes a thickness of ~80 Å (for neon) or ~100 Å (for argon) from the surface.

The influence of thermal treatment under vacuum or with an oxygen leak on XPS analysis was also examined in Table 4 for A2B sample. In fact, a

Table 3. XPS analysis of the yttrium-containing AlN samples

Type	*Chemical formula*		*FWHM (eV)*			*BE(eV)*	
	Before etching	*After etching*	Al_{2p}	O_{1s}	N_{1s}	O_{1s}	N_{1s}
AG35	$AlO_{1.82}N_{0.64}Y_{0.2}$		2·2	3·0	2·0	531·8	396·5
		$AlO_{0.67}N_{0.73}Y_{0.09}$	2·6	3·4	2·2	531·8	396·8
AG75	$AlO_{1.51}N_{0.51}Y_{0.16}$		2·2	3·1	1·9	531·8	397·0
		$AlO_{0.61}N_{0.70}Y_{0.09}$	2·7	3·4	2·2	531·8	397·4
AG250	$AlO_{1.73}N_{0.69}Y_{0.2}$		2·1	2·8	2·0	531·9	396·9
		$AlO_{0.67}N_{0.72}Y_{0.14}$	2·6	3·0	2·4	531·5	396·2

Table 4. Influence of the heating conditions under vacuum on the XPS characteristics of A2B sample

Temperature (°C)	*Chemical formula*	*FWHM (eV)*			*BE (eV)*	
		Al_{2p}	O_{1s}	N_{1s}	O_{1s}	N_{1s}
Room temperature	$AlO_{1.31}N_{0.35}$	2·2	3·1	1·9	531·4	397·1
300	$AlO_{0.95}N_{0.35}$	2·6	2·4	1·6	532·0	397·0
600	$AlO_{1.0}$ $N_{0.36}$	2·6	2·5	1·7	531·7	397·0
600 + O_2 (10^{-6} torr)	$AlO_{1.01}N_{0.38}$	2·7	2·5	1·8	532·0	397·1

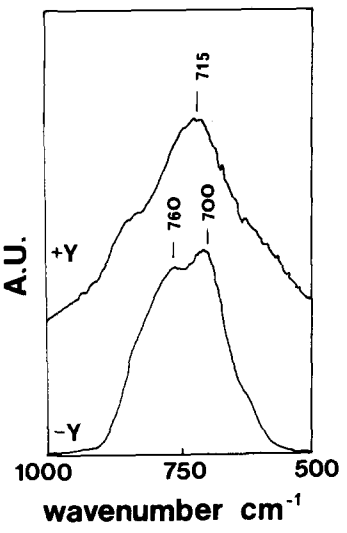

Fig. 4. 500–1000 cm^{-1} spectral range of both yttrium-free (A4) and yttrium-containing (ART AG35) AlN powders.

thermal treatment induces almost the same consequences as an ion bombardment: the superficial quantity of oxygen decreases significantly up to 300°C and, the O_{1s} FWHM decreases, whereas the Al_{2p} FWHM increases upon heating. In contrast, the behaviour of nitrogen in this case cannot be compared to its behaviour during ion bombardment. Indeed, thermal treatment does not affect its superficial concentration, but slightly lowers the FWHM of the N_{1s} line. The setting of an oxygen

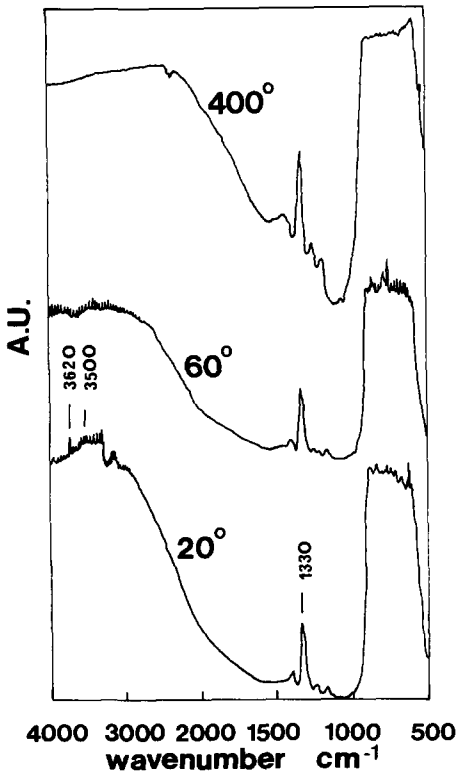

Fig. 5. Influence of the heating conditions on the 400–4000 cm^{-1} spectral range of A2B sample.

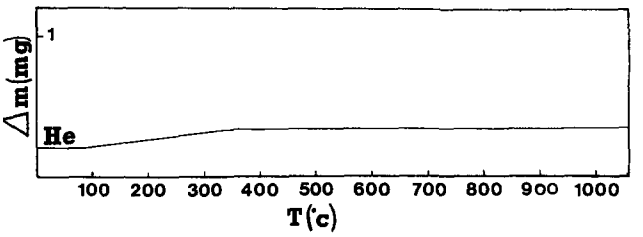

Fig. 6. TGA analysis of A2B sample.

leak at 600°C does not significantly modify these two parameters.

3.3 FTIR

The major IR bands will be successively considered in this section. The IR spectra of all the KBr-dispersed powders (Fig. 4) exhibit a broad intense band at 600–900 cm^{-1}. This band corresponds to stretching vibrations of the Al–N bond.[31] It is striking to note that the maximum of this large band is significantly higher than the value commonly adopted for AlN ($\nu_{Al-N} = 695\,cm^{-1}$). Figure 4 emphasises that yttria-containing AlN powders exhibit still broader bands than yttria-free samples.

The frequency range 3200–3600 cm^{-1} (Fig. 5) was investigated. When submitted to a vacuum (10^{-6} torr) for 12 h, the auto-supported AlN substrates show a great number of very low-intensity peaks in this region. These peaks are found to vanish upon heating to 400°C.

In the spectral range between 1000 and 1600 cm^{-1}, a group of bands, with the most intense one centred at 1330 cm^{-1}, can be seen (Fig. 5). The intensity of these bands decreases as the temperature of the pretreatment increases. Notice that there is no evidence for the familiar deformation band of molecular or crystal H_2O at 1640 cm^{-1}.[31]

3.4 TGA

A thermal treatment up to 1000°C under helium permitted a weight change to be seen (Fig. 6). From 100°C, a small weight loss occurs. This is the only observed variation within the temperature range.

4 Discussion

4.1 XRD

Bulk oxygen levels in AlN powders are far from negligible. Moreover, FTIR has demonstrated that Al–O and O–H bonds exist within the structure of AlN, but, oxide phases are absent from the diffraction patterns. Reasons for this behaviour could be that oxygen exists as a non-crystalline oxide form or that the supposed crystalline form is not

sufficient on a quantitative basis to be detected in the XRD pattern.

4.2 XPS

4.2.1 On the as-received samples, before etching

The permanent occurrence of the Auger oxygen peak as well as the O_{1s} peak shows the presence of oxygen in the most external layers of the nitride grains. In contrast, nitrogen is mostly absent from the uppermost layers (cf. no or very small N Auger signal detected). Detection of N_{1s} in all the cases implies that nitrogen is present under the oxygen-containing layer, the depth of which is of the order of magnitude of the mean free path of the N_{1s} photoelectrons ($\lambda \sim 20$ Å typically).

Some authors[9,16] have assigned abnormally elevated values for the N_{1s} BE of oxidised AlN specimens. Katnani & Papathomas[16] have found that 398·6 eV is the BE of N_{1s} peak, although they have not specified the nature of the reference used for the calibration of the BE scale. Suryanarayana *et al.*,[9] who have studied by XPS silicon nitride-doped (also with Y_2O_3) AlN ceramics, obtained two different signals for the N_{1s} peak, with binding energies equal to 396·6 eV and 399·0 eV. The peak at 396·6 eV, which is the most intense, was assigned to the nitrogen arising from the added Si_3N_4 and the other peak at 399·0 eV to the AlN, reference being made to the work of Katnani & Papanthomas.[16] They also obtained a two-signals N_{1s} band for steam-treated AlN ceramics. The smallest signal at 396·6 eV was attributed to a $SiO_{0.4}N$ form, whereas the largest one at 399·0 eV was assigned to unreacted AlN. Three remarks may be made concerning these conclusions: (1) There is some abnormality in attributing the AlN to the very small intensity peak, and Si_3N_4 to the largest one, even though the sintering additives (<4%) were mixed with AlN, before being blended and fired at 1900°C;[9] (2) the N_{1s} BE of Si_3N_4 is often referred as 398·3 eV in other papers;[24] this value is largely superior to the value proposed by Suryanarayana;[9] (3) for oxidised samples, the peak corresponding to the nitrogen bonded to oxygen appears generally at higher BE values than the peak relative to nitrogen bonded to the metal.[16,28] As a partial conclusion, one can say that nitride-related N_{1s} peaks may be assigned with certainty to lower values, i.e. 396·9 ± 0·2 eV, as was proposed in other works.[28–30]

Oxygen levels which are shown here are important, particularly with regard to the nitrogen values. Many authors[9,13,16] have found similar oxygen to aluminium molar ratios for untreated AlN powders. A distinction has yet to be made between ceramics sintered by conventional methods and by pressureless sintering.[9] Indeed, the O/Al molar ratio obtained in the first case (=3·5) is larger than in the second one (=2·1).

4.2.2 On the as-received samples, after etching

The etching procedure was shown to make the chemical formula of all the samples more or less equivalent, suggesting that the bulk chemical diversity among the samples could arise essentially from the external layers, the inner core being quasi-identical for every powder. Superficial layers, which contain a large quantity of oxygen before etching, become richer in nitrogen in the course of the ion bombardment. It was, however, impossible to reduce the oxygen level to zero with increasing etching times. At this stage, the behaviour could be due to some oxygen reorganisation into superficial layers (pseudo-steady-state conditions). The absence of a modification of the observed surface composition when an oxygen leak is installed should strengthen this assumption. Consequently, the etching procedure has not allowed the thickness of the oxygen-containing layer to be determined.

The decrease of the FWHM of O_{1s} peak in the course of the bombardment could be due to the release of the OH groups present at the surface. This phenomenon, whose occurrence will be demonstrated several times hereafter, would not modify the BE value of the oxygen peak after etching. The increase of the FWHM of N_{1s} and Al_{2p} peaks would be the result of the creation of a large quantity of defects induced by the ionic bombardment.

The large superficial yttrium level, which is linearly related to the oxygen one in the course of the etching procedure, indicates that yttrium is well dispersed on the surface of the grains and there is a gradient of concentration from the uppermost layers to the core of the material.

The thermal treatment up to 600°C causes a large diminution (30%) of the superficial oxygen level. This could be a second proof of the existence of external OH groups. The presumed $Al(OH)_3$ or AlOOH species would be transformed into Al_2O_3 species for temperatures lower than 300°C.

4.3 FTIR

The broadness of the band centred at 700 cm^{-1} may indicate that AlN purity is not high, and particularly that Al–O ($\nu_{Al-O} = 600\ cm^{-1}$) bonds exist within the structure.[11,32] This assumption may be correlated with the known broad absorption band exhibited by aluminium oxide in this region.[31]

It is also well known that the 700 cm^{-1} absorption

band is shifted toward the high-frequency side when AlN is present in an ultradispersed form.[33] For particles having a size range in the order of few micrometers, the very small radius of curvature of the particle surface induces a crystal lattice compression, due to the influence of surface tension forces. As a consequence, this lattice compression generates an increase in the strength of the bond between the aluminium and the nitrogen atoms, and thus in the frequency value of the Al–N bands. This phenomenon was clearly demonstrated by Makarenko *et al.*[11] They have shown that the frequency of the band concerned shifted towards lower values as a result of a high-temperature annealing of ultradispersed AlN powder. A broadening of the same band also occurred under such conditions.

The very large width of the Al–N band for yttrium-containing solids may be attributed to the increased oxygen levels in these samples.

Considering the group of peaks developed in the 3200–3600 cm^{-1} range, these peaks are too small to be ascribed with certainty to hydroxyl groups. Indeed, they could be confused with some noise arising from other factors, but their presence was really confirmed with a further heating at successively 60 and 400°C. The rapid and total disappearance of the peaks indicates that they may really be attributed to superficial OH groups.

The 1330 cm^{-1} band has already been observed by several authors.[14,32] Highfield & Bowen[14] suggested that the strongest line centred at 1330 cm^{-1} could be an overtone of the Al–N stretching fundamental band located at 700 cm^{-1}. By using diffuse-reflectance Fourier Transform infrared spectroscopy (DRIFT) to characterise water-treated AlN, these authors have also observed a band at 1510 cm^{-1}. They assigned this band as the first overtone of the Al–O stretching fundamental, occurring in the range 700–800 cm^{-1}. This band does not appear here. On the other hand, Hoch *et al.*[32] have assigned the band at 1330 cm^{-1} to Al–NH vibrations, where NH vibrates as a single mass. This is, however, in contradiction with the ordinary assignment of NH deformations, localised generally in the spectral range above 1500 cm^{-1}. In the present case, there is evidence of the superficial oxidation of the nitride powders. This phenomenon creates hydroxyl species (Al–OH) on the surface, which are well known to absorb intensively at frequency values lower than 1450 cm^{-1}. Figure 5 shows that these bands vanish progressively upon heating at 60 and 400°C.

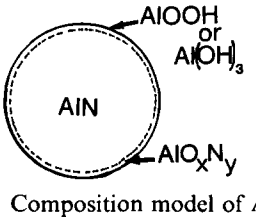

Fig. 7. Composition model of AlN grains.

4.4 TGA

TGA provides one more piece of evidence of the occurrence of easily released species on the surface of AlN grains. These species are strongly presumed to be hydroxyl groups. The smallness of the weight variation would be due to the low number of released hydrolxyl groups, which is a consequence of the small specific area of these powders.

5 Conclusion

Hydroxyl species, easily releasable by a thermal treatment or an ionic bombardment, are superficially present on AlN grains. They result from a superficial oxidation process under ambient conditions. This transformation alters more than superficial layers. Indeed, Al–O bonds are also found to exist within the structure, besides Al–N bonds. Moreover, a pure AlN hexagonal structure is detected by XRD.

An illustrative scheme representing a composition model of AlN grains may be deduced from these results (Fig. 7). In this model, an oxynitride-type phase (of average formula $AlO_{0.5}N_{0.6}$) would form an intermediate layer between the nitride core and the external oxyhydrated phase (AlOOH, $Al(OH)_3$). Notice that the oxynitride-type phase is not a well-defined AlON phase, due to the fact that oxygen species diffuse within the AlN framework.

Acknowledgment

The authors thank the European Community (EEC) for providing funds in the frame of a BRITE-EURAM program, Contract No. BREU-0055-C.

References

1. Suryanarayana, D., Thermally conductive ceramics in electronic packaging. *J. Electron. Packag.*, **111** (1989) 192.
2. Iwase, N., Anzai, K. & Shinozaki, K., AlN substrates having high thermal conductivity. *Solid State Technol.*, Oct. (1986) 135.
3. Borom, M. P., Slack, G. A. & Szymaszek, J. W., Thermal

conductivity of commercial AlN. *Ceramic Bulletin*, **51**(11) (1972) 852.
4. Slack, G. A., Nonmetallic crystals with high thermal conductivity. *J. Phys. Chem. Solids*, **34** (1973) 321.
5. Sakai, T. & Iwata, M., Effect of oxygen on sintering of AlN. *J. Mater. Sci.*, **12** (1977) 1659.
6. Witek, S. R., Miller, G. A. & Harmer, M. P., Effects of CaO on the strength and toughness of AlN. *J. Am. Ceram. Soc.*, **72**(3) (1989) 469.
7. Sakai, T., Effect of oxygen composition on flexural strength of hot-pressed AlN. *J. Am. Ceram. Soc.*, **61**(9–10) (1978) 460.
8. Kluge-Weiss, P. & Gobrecht, J., Directly bonded copper metallization of AlN substrates for power hybrids. *Mater. Res. Soc. Symp. Proc.*, **40** (1985) 399.
9. Suryanarayana, D., Matienzo, L. J. & Spencer, D. F., Behavior of AlN ceramic surfaces under hydrothermal oxidation treatments. *IEEE Trans. Compon. Hybrids Manuf. Technol.*, **12**(4) (1989) 566.
10. Kurihara, Y., Endoh, T. & Yamada, K., The influence of moisture on surface properties and insulation characteristics of AlN substrates. *IEEE Trans. Compon. Hybrids Manuf. Technol.*, **12**(3) (1989) 330.
11. Makarenko, G. N., Zyatkevich, D. P., Arsenin, K. I., Karlysheva, K. F., Kosolapova, T. Ya. & Sheka, I. A., IR spectra of ultradispersed AlN powder. *Inorg. Mater.*, **15**(4) (1979) 535.
12. Sato, T., Haryu, K., Endo, T. & Shimada, M., High temperature oxidation of hot-pressed AlN by water vapour. *J. Mater. Sci.*, **22** (1987) 2277.
13. Bowen, P., Highfield, J. G., Mocellin, A. & Ring, T. A., Degradation of AlN powder in an aqueous environment. *J. Amer. Ceram. Soc.*, **73**(3) (1990) 724.
14. Highfield, J. G. & Bowen, P., DRIFT studies of the stability of AlN powder in an aqueous environment. *Anal. Chem.*, **61** (1989) 2399.
15. Chanchani, R., Processability of thin-film, fine line pattern on AlN substrates. *IEEE Trans. Compon. Hybrids Manuf. Technol.*, **11**(4) (1988) 427.
16. Katnani, A. D. & Papathomas, K. I., Kinetics and initial stages of oxidation of AlN: TGA and XPS study. *J. Vacuum Sci. Technol. A*, **5**(4) (1987) 1335.
17. Suryanarayana, D., Oxidation kinetics of AlN. *J. Am. Ceram. Soc.*, **73**(4) (1990) 1108.
18. Billy, M., The kinetics of gas–solid reactions and environmental degradation of nitrogen ceramics. In *Progress in Nitrogen Ceramics*, ed. F. L. Riley. M. Nijhoff, Boston, MA, 1983, p. 403.
19. Billy, M., Jarrige, J., Lecompte, J. P., Mexmain, J. & Yefsah, S., Comportement à l'oxidation du nitrure d'Al fritté. *Rev. Chim. Minérale*, **19** (1982) 673.
20. Lefort, P., Ado, G. & Billy, M., Oxydation de l'oxynitrure d'Al pulvérulent dans l'O_2 au dessus de 1100°C. *Ann. Chim. Fr.*, **14** (1989) 227.
21. Yagi, T., Shinozaki, K., Ishizawa, N., Mizutani, N. & Kato, M., Effect of SiO_2 on the thermal diffusivity of AlN ceramics. *J. Amer. Ceram. Soc.*, **71**(7) (1988) 334.
22. Lavrenko, V. A. & Alexeev, A. F., Oxidation of sintered AlN. *Ceram. Int.*, **9**(3) (1983) 80.
23. Abid, A., Bensalem, R. & Sealy, B. J., The thermal stability of AlN. *J. Mater. Sci.*, **21** (1986) 1301.
24. Bergström, L. & Pugh, R. J., Interfacial characterisation of silicon nitride powders. *J. Amer. Ceram. Soc.*, **72**(1) (1989) 103.
25. Grimblot, J. & Eldridge, J. M., Influence of the growth conditions of Al_2O_3 passivating layers on the corrosion of aluminum films in water. *J. Electrochem. Soc.*, **128** (1981) 729.
26. Wagner, C. D., Passoja, D. E., Hillery, H. F., Kinisky, T. G., Six, H. A., Jansen, W. T. & Taylor, J. A., Auger and photoelectronc line energy relationships in Al–O and Si–O compounds. *J. Vacuum Sci. Technol.*, **21**(4) (1982) 933.
27. Scofield, J. H., Hartree–Slater subshell photoionization cross-sections at 1254 and 1487 eV. *J. Elect. Spect. Rel. Phenom.*, **8** (1976) 129.
28. Kovacich, J. A., Kasperkiewicz, J., Lichtman, D. & Aita, C. R., Auger electron and XPS of sputter deposited AlN. *J. Appl. Phys.*, **55**(8) (1984) 2935.
29. Taylor, J. A., & Rabalais, J. W., Reactions of N_2^+ beams with aluminum surfaces. *J. Chem. Phys.*, **75**(4) (1981) 1735.
30. Raole, P. M., Prabhawalkar, P. D., Kothani, D. C., Pawar, P. S. & Gogawale, S. V., XPS studies of N^+ implanted aluminum. *Nuclear Inst. Meth. Phys. Res.*, **B23** (1987) 329.
31. Nyqist, R. A. & Kagel, R. O., Infrared spectra of inorganic compounds. Academic Press, New York, 1971, p. 495.
32. Hoch, M., Vernardakis, T. & Nair, K. M., Ultrafine powders of AlN, Si_3N_4 and sialons: an IR study. *Sci. Ceram.*, **10** (1980) 227.
33. Morokhov, I. D., Trusov, L. I. & Chizhik, S. P., Ultradispersed metallic media. Atomizdat, Moscow, 1977. (In Russian.)